Finite wave vector Jahn-Teller pairing and superconductivity in the cuprates

D. Mihailovic and V. V. Kabanov
Jozef Stefan Institute, Jamova 39, 1001 Ljubljana, Slovenia
(Received 18 January 2000; revised manuscript received 20 July 2000; published 3 January 2001)

A model interaction is proposed in which pairing is caused by a *nonlocal* Jahn-Teller-like instability due to the coupling between planar O states and $k \neq 0$ phonons. Apart from pairing, the interaction is found to naturally allow metallic stripe formation. The consequences of the model for superconductivity in the cuprates are discussed. The model is shown to be consistent with numerous sets of experimental data in quite some detail.

DOI: 10.1103/PhysRevB.63.054505 PACS number(s): 74.20.−z, 74.25.−q, 74.72.−h

I. INTRODUCTION

A Jahn-Teller (JT) polaron pairing effect was originally proposed as a possible explanation for the superconductivity in $La_{2-x}Ba_xCuO_4$ by Bednorz and Müller.[1] Since then, the JT effect has been discussed by a number of authors in different contexts[2–6] and although many features have been observed experimentally supporting the general concept of JT polarons,[7,8] so far no generally applicable model has been shown to be compatible with the overall phenomenology observed in the cuprates. One of the major problems is that the single-ion JT energy splitting between Cu $d_{x^2-y^2}$ states and $d_{3r^2-z^2}$ states is thought to be of the order of 1 eV or more, too large to play a role in the pseudogap physics, which is believed to be the energy scale of the pairing interaction, which is of the order of 0.1 eV. Nevertheless, the observation of a large isotope effect on both T_c (Ref. 9), T^* (Ref. 8) and penetration depth[10] firmly establishes a role for lattice polarons in the pairing mechanism, while the fact that a depression in the spin susceptibility usually appears at a lower temperature than the ''pseudogap'' observed by charge excitation spectroscopies[11,12] suggests that a lattice pairing mechanism is primary and the spin ordering follows.

In this paper, we outline a microscopic pairing scenario in $La_{2-x}Sr_xCuO_4$ driven by a finite wave vector JT instability. We find that the proposed model can explain many of the general features both in the underdoped and overdoped regions of the phase diagram and is fundamentally compatible with the overall phenomenology of the cuprates.

The experimental observations on which the present scenario is based are mainly those showing evidence for the existence of dynamic incommensurate lattice distortions associated with doped holes. Inelastic neutron scattering,[11,13] neutron pair distribution function (PDF), [14] extended x-ray-absorption fine structure (EXAFS),[15,16] and electron-spin-resonance (ESR)[17] experiments all show the existence of dynamic lattice distortions on time scales relevant for pairing of 10^{-13}–10^{-15} s. The inelastic neutron scattering data[13,11] can be singled out for *directly* giving not only the energy, but also the wave vector associated with the lattice distortion and its range in k space without any interpretation or modeling. The observed distorted regions appear to be along the $(\zeta,0,0)$ [or $(0,\zeta,0)$] directions and have typical dimensions in real space of $2a \times 5a (8 \times 20$ Å), where a is the lattice constant. A schematic diagram of the distortion derived from an analysis of the data is shown in Fig. 1. The energy of the anomaly of $E_a = 65$–85 meV is of the order of the ''pseudogap'' energy, while its width of $\Delta E \simeq 5$ meV corresponds closely to the linewidth expected from the measured pair recombination rate, $h/\pi c\tau \simeq 4$ meV.[18] At the doping level of $x = 0.15$, the two-dimensional (2D) volume of the object in Fig. 1 contains approximately 1.5 carriers. Taken together, the implication is that the objects can be interpreted as k-space ''snapshots'' of individual pairs.

Additional experimental observations that we consider important in the present context are evidence for the coexistence of two carrier types in a large part of the phase diagram,[19,20] and—in addition to the ''pseudogap''—the appearance of a temperature-dependent superconducting gap $\Delta_c(T)$, which closes at T_c (Refs. 21 and 18) that is particularly well observed at higher doping levels and has a magnitude at $T=0$ of $\Delta_c(0) \lesssim \Delta_p$.

II. JT PAIRS AND STRIPES

Before proceeding with the analysis of the e-p coupling for the case of general k, let us briefly discuss the Γ-point coupling ($k=0$) in the tetragonal group D_{4h}^{17} ($I4/mmm$) applicable to $La_{2-x}Sr_xCuO_4$. The symmetrized cross product of the representations at the Γ point is

$$[E_u \times E_u] = [E_g \times E_g] = A_{1g} + B_{1g} + B_{2g}, \qquad (1)$$

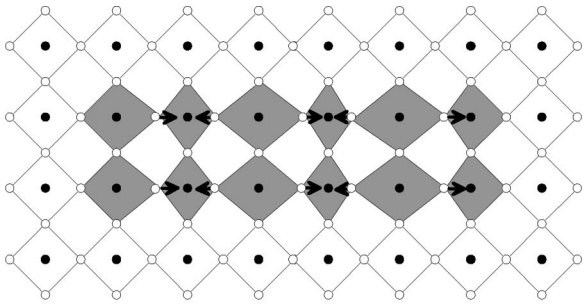

FIG. 1. The distortion in the Cu-O plane corresponding to the anomalous mode observed in inelastic neutron scattering in $La_{2-x}Sr_xCuO_4$ (Refs. 13 and 11). The O displacements are those of the τ_1 mode shown in Fig. 3 and, in general, have different phases.

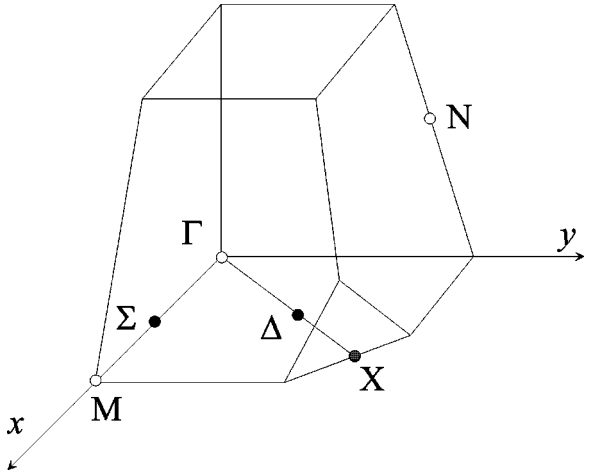

FIG. 2. The Brillouin zone (BZ) of $La_{2-x}Sr_xCuO_4$ corresponding to the tetragonal phase with point group D_{4h}.

which contains no degenerate representations. On the other hand, the lattice vibrations at the Γ point transform as

$$\Gamma = 2A_{1g} + 4A_{2u} + B_{2u} + 2E_g + 5E_u .$$

Since there are no B_{1g} and B_{2g} representations at the Γ point, electrons can couple only with A_{1g} phonon modes. In D_{4h} there are two such modes associated with apex oxygens or La ions. However, the experiments show that the modes involved in the intraction are those of in-plane O atoms, which do not couple at the Γ point. This leads us to the main conjecture of the proposed pairing model, namely, the existence of *intersite* pairs that form via a $k \neq 0$ interaction.

The existence of intersite pairs in cuprate superconductors is inferred from their very short coherence length. Given that the pair dimensions l_p cannot exceed the coherence length, i.e., $l_p \lesssim \xi$, we may infer that any possible lattice distortions associated with pairing have a finite range $\sim l_p$. The effect of such lattice distortions should also be evident in reciprocal space with an anomaly centered around a wave vector $k \simeq 1/l_p$. Following the inelastic neutron-scattering data[13] that shows an anomaly approximately at $k_0 \simeq [\pm \pi/2a, 0, 0]$ extending over almost half the Brillouin zone (BZ) $\Delta k \sim 1/2a$, we can write the electron-phonon interaction for such an object in the form

$$g(k_0,k) = g_0/[(k-k_0)^2 + \gamma^2], \tag{2}$$

where g_0 is a constant describing the strength of coupling and k_0 defines the wave vector associated with the interaction and its range in k space, which—neglecting fluctuations—also defines its extent in real space (interhole spacing) as $l_p \sim k_0^{-1}$. $\gamma = \Delta k$ defines its width in k space and gives the width of the distribution of intercarrier distances within the interacting pair. This is related to the average size of the deformation of each particle in real space γ^{-1}.

We now proceed with an analysis of the e-p coupling using group theory for $k \neq 0$ intersite pairing and first discuss the relevant phonon modes. The BZ corresponding to the tetragonal space group D_{4h}^{17} applicable for $La_{2-x}Sr_xCuO_4$ is shown in Fig. 2. To consider local pairs and/or stripes forming along the Cu-O bond direction or along 45° to it, we need to consider the general wave vector Σ and the Δ points, corresponding to the $(\zeta,0,0)$ and $(\zeta,\zeta,0)$ directions, respectively. [The special symmetry points (Γ, X, and M, etc.) give rise to commensurate distortions that will be discussed later.] The relevant lattice deformation associated with the neutron mode at 75 meV (Ref. 13) (Fig. 1) is of τ_1 symmetry, where τ_1 is the irreducible representation of the little group corresponding to the Σ direction in the BZ as shown in Fig. 3. Since in principle all modes of τ_1 symmetry can couple to electrons, for completeness we show all the possible modes with τ_1 symmetry in Fig. 3. However, the most relevant mode—i.e., the one for which the anomaly is observed to be most pronounced—involves in-plane O1 displacements along the Cu-O bonds (see also Fig. 1).

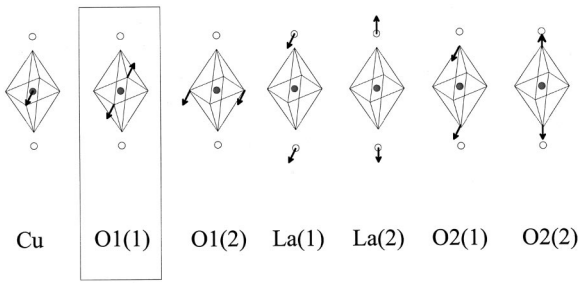

FIG. 3. The ionic displacements in $La_{2-x}Sr_xCuO_4$ corresponding to τ_1 symmetry of the little group at the Σ point in the BZ. The mode observed in neutron scattering corresponds to the O1(1) displacements.

A. $k \neq 0$ phonon coupling to nondegenerate electronic states

Since the Σ point has a four-pronged star in D_{4h}, the coupling of electrons in single nondegenerate electronic states to $k \neq 0$ phonons can be written as

$$H_{int} = \sum_{\mathbf{l},s} n_{\mathbf{l},s} \sum_{k_0=1}^{4} \sum_{\mathbf{k}} g(k_0,\mathbf{k}) \exp(i\mathbf{kl})(b^{\dagger}_{-\mathbf{k}} + b_{\mathbf{k}}), \tag{3}$$

where $\mathbf{l}$ is the site label, and

$$g(k_0,\mathbf{k}) = g(\pi\gamma^2)^{1/2}/((k-k_0)^2 + \gamma^2), \tag{4}$$

where k_0 are the four wave vectors corresponding to the prongs of the star associated with the interaction. The nondegenerate electronic states in this interaction allowed by symmetry are associated with p_z orbitals of planar oxygens and transform as A_{2u} or B_{2u} representations of the D_{4h} symmetry group. However, the Hamiltonian (3) above on its own does not lead to symmetry breaking, and thus is not of direct relevance for pair or stripe formation.

B. $k \neq 0$ phonon coupling to degenerate electronic states (Jahn-Teller-like pairing)

A more interesting case arises when twofold degenerate levels (for example, the two E_u states corresponding to the planar O p_x and p_y orbitals or the E_u and E_g states of the apical O) interact with $k \neq 0$ phonons. We are particularly interested in the phonons that lead to symmetry breaking and

allow the formation of intersite pairs or stripes. In Eq. (5), we give the invariant Hamiltonian that couples degenerate electronic states to phonons transforming as the τ_1 representations of the group of wave vectors G_k. Taking into account that E_g and E_u representations are real, and Pauli matrices σ_i corresponding to the doublet of E_g or E_u transform as A_{1g} $(k_x^2+k_y^2)$ for

$$\sigma_0=\begin{pmatrix}1 & 0\\ 0 & 1\end{pmatrix},$$

B_{1g} $(k_x^2-k_y^2)$ for

$$\sigma_3=\begin{pmatrix}1 & 0\\ 0 & -1\end{pmatrix},$$

B_{2g} (k_xk_y) for

$$\sigma_1=\begin{pmatrix}0 & 1\\ 1 & 0\end{pmatrix},$$

and A_{2g} (s_z) for

$$\sigma_2=\begin{pmatrix}0 & -i\\ i & 0\end{pmatrix}$$

representations, respectively, an invariant Hamiltonian is given by

$$\begin{aligned}H_{int}=&\sum_{\mathbf{l},s}\ \sigma_{0,\mathbf{l}}\sum_{k_0=1}^{4}\ \sum_{\mathbf{k}}\ g_0(k_0,\mathbf{k})\exp(i\mathbf{kl})(b^{\dagger}_{-\mathbf{k}}+b_{\mathbf{k}})\\ &+\sum_{\mathbf{l},s}\ \sigma_{3,\mathbf{l}}\sum_{k_0=1}^{4}\ \sum_{\mathbf{k}}\ g_1(k_0,\mathbf{k})(k_x^2-k_y^2)\\ &\times\exp(i\mathbf{kl})(b^{\dagger}_{-\mathbf{k}}+b_{\mathbf{k}})\\ &+\sum_{\mathbf{l},s}\ \sigma_{1,\mathbf{l}}\sum_{k_0=1}^{4}\ \sum_{\mathbf{k}}\ g_2(k_0,\mathbf{k})k_xk_y\exp(i\mathbf{kl})(b^{\dagger}_{-\mathbf{k}}+b_{\mathbf{k}})\\ &+\sum_{\mathbf{l},s}\ \sigma_{2,\mathbf{l}}S_{z,\mathbf{l}}\sum_{k_0=1}^{4}\ \sum_{\mathbf{k}}\ g_3(k_0,\mathbf{k})k_0^2\exp(i\mathbf{kl})(b^{\dagger}_{-\mathbf{k}}+b_{\mathbf{k}}),\end{aligned}\tag{5}$$

where

$$g_i(k_0,\mathbf{k})=g_i(\pi\gamma^2)^{1/2}/[(k-k_0)^2+\gamma^2].\tag{6}$$

The first term in Eq. (5) describes symmetric coupling and is identical to the nondegenerate case [Eq. (3)]. The second and third terms describe the *e-p* interaction corresponding to the Σ and Δ directions, respectively, while the last term describes the *coupling to spins*.[22].

The proposed interaction (5) on its own, results in a splitting of the degenerate states, breaking the tetragonal symmetry and resulting in a local orthorhomb ic distortion at k_0 extending over γ in k space. It can, therefore, lead to the formation of bound intersite pairs and/or stripes with no further interactions. Of course the stability and size of such a distortion will be determined by the balance of short-range attraction, long-range Coulomb repulsion, and kinetic energy.[23]

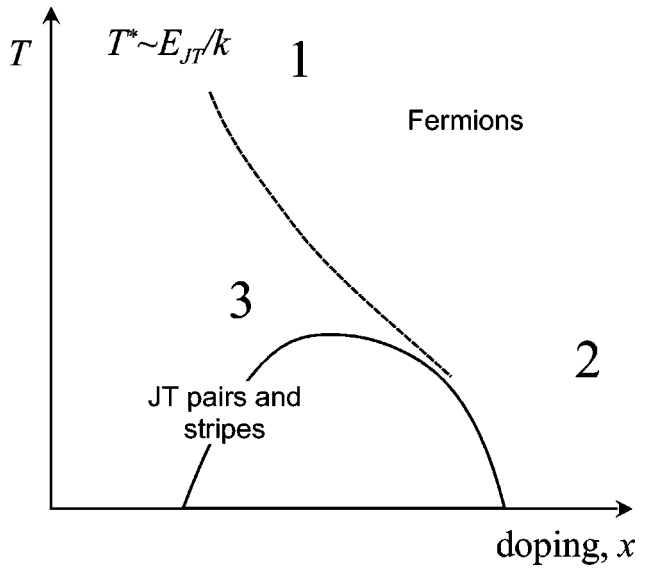

FIG. 4. A schematic phase diagram suggested on the basis of the proposed model for the cuprates. The dashed line indicates the temperature T^*, where $kT^*\simeq E_{JT}$. The solid line indicates the temperature T_c of the onset of macroscopic phase coherence and is given by Eq. (7).

Now let us discuss the properties of the system governed by this Hamiltonian [Eq. (5)]. The importance of the different terms is of course to be determined by experiments. For example, the large 20% anomaly in inelastic neutron scattering at the Σ point clearly emphasizes the second (d-wave) term, while the absence of strong anomalies at $k=0$ deemphasizes the symmetric (s-wave) term and so the new ground state is expected to be a pair that extends over a few unit cells along the Cu-O bond direction $(\pm\zeta,0,0)$ or $(0,\pm\zeta,0)$.[24] The internal lattice structure within the pair is distorted, so pairing would be associated with a reduced *local* symmetry within the pair. In other words, the tetragonal or pseudotetragonal symmetry of the crystal is broken locally by the formation of a nonlocal JT pair with a binding energy E_{JT} given by the solution to the Hamiltonian (5). We thus associate the pairing energy gap E_{JT} with the experimental observation of a ''pseudogap'' at $kT^*\sim\Delta_p=E_{JT}$.[12,18]

To understand these finite wave vector JT pairs in the context of the phase diagram of the cuprates, we consider the effect of thermal fluctuations as the temperature is reduced through T^* in the underdoped phase (Fig. 4). For $T>T^*$ thermal energy prevents the carriers from forming pairs at all levels of doping (shown schematically in the top row in Fig. 5). Approaching T^*, JT pairs start to form and exist in equilibrium with unbound carriers according to chemical balance at thermodynamic equilibrium $n_{unbound}\sim\exp[-E_{JT}/k_BT]$ and shown schematically in the lower panel of Fig. 5(b). [The doping dependence of Δ_p, which is observed to approximately follow an inverse law $\Delta_p\sim 1/x$ (Refs. 19, 18, and 25) is suggested to be a result of screening as discussed by Alexandrov, Kabanov, and Mott,[26] and will not be discussed further here.]

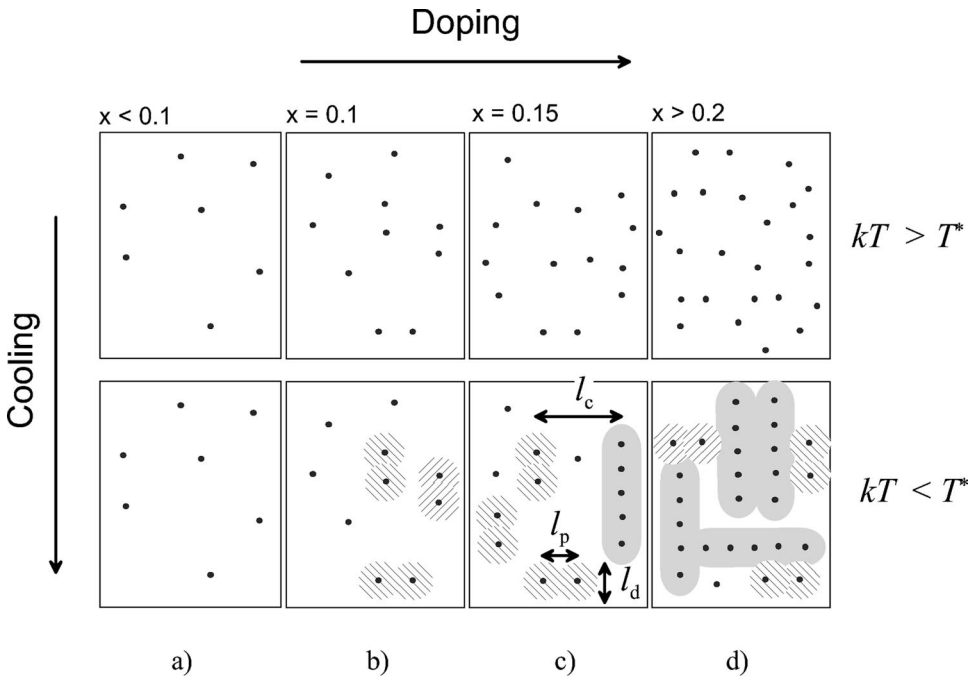

FIG. 5. Real-space schematic diagram representing approximately 100 unit cells ($\approx 4\xi^2$) in the Cu-O plane at different doping levels: (a) for $T > T^*$, the carriers are unbound single particles (region 1 in the phase diagram in Fig. 4) and (b) for $T < T^*$ in the underdoped state (region 3 in Fig. 4), pairs and unbound particles coexist with few stripes. For $T < T^*$ near optimum doping and in the overdoped state, (c) and (d), respectively, pairs coexist with unbound particles and stripes.

For such nonlocal pairs to be stable, the energy gained by the JT pairing must counteract the Coulomb repulsion between two charge carriers within the pair $E_{JT} \gtrsim V_i$. The *upper limit* for the Coulumb repulsion between two carriers approximately one coherence length apart is given by $V_i = e^2/4\pi\varepsilon r \simeq 0.3$ eV [taking $r = r_0 \cong \hbar/k_0 \cong 1$ nm $\lesssim \xi_s$ and $\varepsilon = 4$ (Ref. 27)]. However, since $\varepsilon(\omega) \gg 4$ in the relevant frequency range for pairing (1–4 THz),[27] the relevant value of V_i can be significantly smaller and can be easily overcome by E_{JT}.

Once preformed bosonic pairs exist, superconductivity can occur when phase fluctuations between these pairs are sufficiently reduced so that phase coherence can be established between them. This can occur by Bose condensation[28–30] or some form of the Kosterlitz-Thouless transition.[31,32] In both cases the critical transition temperature in the underdoped region of the phase diagram is given by an expression relating T_c to the pair density n_p and effective mass m^*:

$$T_c \simeq \hbar^2 n_p^{2/D}/(2m^*)k_B, \tag{7}$$

where D is the dimensionality of the system.[33] An important issue related to whether Bose condensation occurs or another mechanism is responsible for the formation of the condensate formation is the number of pairs per coherence volume V_ξ. Using the experimental upper limit of coherence length in $La_{1.85}S_{0.15}CuO_4$ at $T=0$ of $\xi \simeq 20$ Å and assuming for the moment a uniform carrier density in the Cu-O planes, then at a carrier concentration of $x=0.15$ there are approximately 1.5 *pairs per coherence volume*. Considering the experimental error and uncertainties in geometrical factors involved in determining ξ, it is clear that a crossover seems to occur near optimum doping from $n_p < 1$ per V_ξ to $n_p > 1$ per V_ξ, implying a crossover from a Bose condensation to an overlapping-pair superconductivity scenario.[29] Importantly, both are consistent with the finite-wave vector nonlocal JT-pairing interaction described here. (The detailed mechanism for the formation of a phase-coherent condensate is not the subject of the present paper and will not be discussed further here.)

C. Stripes

So far, the discussion concerned a intersite pairing-JT effect with two particles involved. If more than two particles are involved in the interaction, the effect of Eq. (5) is similar and provided $k_0 > \gamma$ [Eq. (1)], a JT distortion can occur along a stripe, for example. The internal *lattice* structure of such stripes is defined by the JT lattice distortion, just as for pairs. The shape of these objects is determined primarily by minimization of the Coulomb energy, and the formation of 1D stripes is clearly more favorable than 2D clusters in this respect.[23] The incommensurability of the dynamic JT distortion given by k_0 means that the number of sites in the stripe is larger than the number of carriers, resulting in a partially filled ground state. The electronic wave function inside such stripes is *extended*, that is, it extends throughout the entire stripe, and the macroscopic transport properties in the normal state are thus expected to be dominated by hopping or tunneling of carries *between* the stripes, rather than within them. The elementary excitations of such objects are expected to be Fermionic and metallic in character, which makes their statistics different than for the JT pairs, which are bosons. The JT stripes are expected to *coexist* both with JT pairs *and* unbound particles, with their relative populations determined by chemical balance and the pair binding energy E_{JT} compared to the stripe formation energy. A schematic real-space ''snapshot'' of this phase is shown in Fig. 5(c). Note that because we have a four-pronged star for the Σ-point distortions, four different types of stripes can form, each corresponding to one of the four k_0. Since the little group at the Σ

point does not have inversion symmetry, the stripes can have a local polarization (i.e., have a ferroelectric phase). This may explain the presence of a spontaneous polarization in these materials and the appearance of a pyroelectric effect in $La_{2-x}Sr_xCuO_4$ (Ref. 34) and other cuprates.[35]

A most simple and appealing possibility is that superconductivity in the presence of stripes still occurs via the same preformed pair scenario as discussed in the previous section. However, the stripes then appear to have a detrimental effect on superconductivity because they take up carriers and thus reduce the number of pairs.

III. OVERDOPED REGIME

As the density of doped holes increases with increasing doping, the spacing between them becomes comparable to the pair size and they start to overlap, so interactions between the pairs and stripes become important, and some kind of collective or cooperative effect that extends over both types of objects needs to be considered.

The Hamiltonian in Eq. (5) introduces a number of length scales [see Fig. 5(c)]. The first is the mean distance between the charge carriers in the pair (or within the stripe) $l_p \simeq 1/k_0$. The second is the length of the stripes l_s and finally, there is the length scale l_c, describing the characteristic distance *between* the pairs or stripes, which is determined simply by the carrier density.

With increasing doping, the distance between the pairs and stripes l_c decreases, and increased screening reduces Coulomb repulsion, which in turn leads to increased stripe length l_s. At some point, l_c becomes comparable to the superconducting coherence length ξ_s, and the pairs become *proximity coupled* to the metallic stripes [Fig. 5(c)]. In other words, superconductivity in the stripes will be induced below T_c by a JT pair-gap proximity effect. Above T_c, there is no proximity coupling, and so clearly, the superconducting order parameter must be zero in the stripes. Thus, it is evident that the superconducting gap has to be T dependent within the stripes. This presents an explanation for the experimentally observed *coexistence* of a T-independent pairing gap (''pseudogap'') E_{JT} and a T dependent superconducting gap $\Delta_s(T)$[18,21,36] for which $\Delta_s(0) \lesssim E_{JT}$.

The proposed model suggests a simple explanation why T_c *decreases* in the overdoped regime. With increased doping, the stripe length l_s increases, leading to increased overall metallicity, while at the same time, *the number of pairs decreases*, leading to a decrease in T_c according to the formula given by Eq. (8). Eventually in the metallic, nonsuperconducting phase, $l_c \lesssim l_p$, and the material becomes a homogeneous metal with no pairs and hence, the phase no longer supports high-temperature superconductivity.

Above T^* the crossover from the underdoped to the overdoped phase manifests itself in a change of nondegenerate to degenerate statistics, as indicated by region 1 and region 2, respectively, in the phase diagram in Fig. 4. In principle, they should be distinguishable from the temperature dependence of the susceptibility, for example, which should be Curie-like in region 1 and Pauli-like in region 2, particularly at low temperatures (see Fig. 4). In contrast, the crossover from region 1 to 3 is governed by excitations across the pseudogap with the temperature dependence of the susceptibility given by $\chi(T) \propto 1/T^{\alpha} \exp[-E_{JT}/kT]$.[26,19,12]

IV. DISCUSSION

An important issue that needs to be discussed is the effective mass of the nonlocal JT pairs coupled by $k \neq 0$ wave vector phonons. Let us consider—for simplicity—only the most experimentally relevant interaction for Σ-point coupling, i.e., the $(k_x^2 - k_y^2)$ term of the Hamiltonian Eq. (5). In this case, we can apply the Lang-Firsov[37] transformation, which will give an appropriate estimate of the particle mass.[38] In that case, the effective mass renormalization is exponential:

$$\frac{m^*}{m_0} = \exp(g_{eff}^2), \tag{8}$$

where m_0 is the bare electron mass, and

$$g_{eff}^2 = \frac{1}{(2\pi)^2} \int d^2k g_k^2 [1 - \cos(ka)]. \tag{9}$$

For simplicity, here the integration is carried over the $Cu\text{-}O_2$ plane, so k refers to in-plane momentum. Assuming that the main contribution comes from $k \simeq k_0$, ignoring the effect of γ and integrating, we obtain

$$g_{eff}^2 = g^2 k_0^4 [1 - \cos(k_0 a)]/8\pi. \tag{10}$$

This formula can be rewritten in terms of the ground-state energy of a single polaron as

$$g_{eff}^2 = \frac{E_p[1 - \cos(k_0 a)]}{2\omega}, \tag{11}$$

where the polaron binding energy $E_p = g^2 k_0^4 \omega/4\pi$. When compared with the similar expression for the effective mass in the Holstein model, which has no k dependence, we find that the effective-mass exponent is a factor 2 smaller than the corresponding expression in the Holstein (bi)polaron.[39] If $k_0 < \pi/2a$, the effective mass becomes even smaller, reflecting the fact that for forward scattering, the electron-phonon interaction does not increase the mass strongly. Indeed for $k_0 \to 0$, the effective mass approaches the bare electron mass $m^* \to m_0$. This effect is similar to that discussed by Alexandrov for the case of the Froehlich interaction.[40] However, note that in this case, the interaction is weak and there is no pair binding at all for $k = 0$, which means that it is not relevant if we are considering pairing, but *is* relevant if we consider single-electron transport in the normal state. On the other hand, if $k_0 > \pi/2a$, the mass enhancement becomes more pronounced because of strong backscattering, and so at the zone boundary, corresponding to the special points X and M in the BZ, we expect a very large coupling and a strongly enhanced pair mass. This situation would be relevant to a zone doubling (for the M point) or quadrupling (for the X point) charge-density wave (CDW) formation and/or the for-

mation of long-range order associated with a structural phase transition. The case *relevant for pairing* is of course intermediate, as indicated by the wave vector k_0 in the neutron experiments.

As already discussed, according to the neutron data, the interaction in the cuprates appears to take place over a large range of wave vectors γ centered near $k_0 \sim 1/l_p$. An interesting case arises at the 1/8 doping level, where the interparticle distance $l = \sqrt{8}a$. If l corresponds exactly to $l = 2\pi/k_0$, we expect to observe a CDW with a periodicity given by k_0. (Note that this is different to the simpler case of a zone-boundary CDW discussed in the previous paragraph.)

In the underdoped state, the JT model is different from the bipolaronic models[28,41] and other intersite models[42] primarily with regard to the detailed mechanism of bipolaron formation. Whereas the standard bipolaron model usually refers to quantum-chemical calculations[42] and does not necessarily involve a particular JT mode nor a specific local symmetry change upon pairing, the present intersite JT pairing model does so, and implies a very specific Hamiltonian [Eq. (5)] that is based on the symmetry analysis of experimentally determined local distortions. Equation (2) at first sight has some common features with the phenomenology of the CDW scenario.[43] The present model offers a microscopic description for the origin of this interaction as arising from JT coupling between a $k \neq 0$ mode and degenerate electronic states.

The proposed scenario suggests the coexistence of Fermionic excitations in stripes and bosons (pairs) over the entire phase diagram in different proportion determined by thermodynamic equilibrium. This appears to be born out by the susceptibility data[19] and the two-component interpretation of the optical conductivity,[27,44] amongst others.[45]

It can also be shown to be consistent with the temperature and doping dependence of angle-resolved photoemission spectra. A pairing JT deformation at the Σ point leads to objects that have finite dimensions along the *a* or *b* crystal axes. We therefore expect to observe features associated with these objects in *k* space along the Σ direction (i.e., along the Γ-*M*) and the appearance of a ''pseudogap'' in the angle-resolved photoemission spectroscopy (ARPES) spectra. The range of wave vectors where such a ''pseudogap'' appears is given by $\Delta k \sim \gamma$ from Eq. (1). In the metallic stripes, on the other hand, in which Fermionic excitations exist in the normal state, above T_c we expect to observe a band that crosses the Fermi level along the Σ direction. Importantly, with increased carrier concentration, the increased *coupling between pairs and stripes* leads to increased 2D order, progressively extending the Fermi surface in the overdoped state. Clearly, the temperature-dependent superconducting gap $\Delta_s(T)$ that forms in the stripes will appear in the same regions in *k* space as the Fermionic band. If we assume that the model can be extended to $Bi_2Sr_2CaCu_2O_{8+\delta}$, the coexistence of a *T*-dependent ''superconducting'' gap and a ''pseudogap'' along Γ-*M* [i.e., the Σ direction (see Fig. 2)], and especially the apparent ''destruction of the Fermi surface'' with underdoping[21] can be understood to be a consequence of the Hamiltonian Eq. (5).

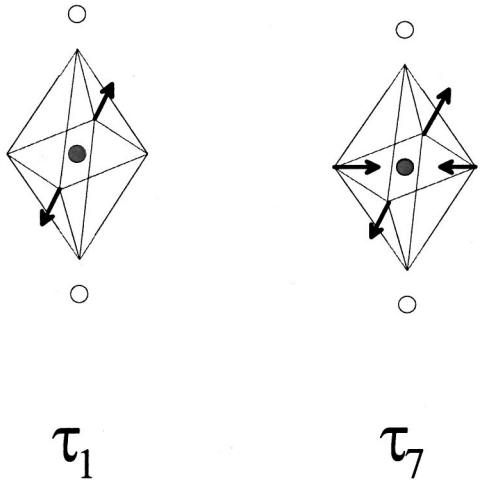

FIG. 6. A superposition of two τ_1 modes [observed in neutron scattering by McQueeney *et al.* (Ref. 13)] with orthogonal *k* vectors at the Σ point has the same displacements as the τ_7 mode at the zone boundary observed in ESR (Ref. 17).

Reconciling the slight differences in the interpretation of the observed lattice distortions in ESR, EXAFS, and inelastic neutron scattering, the Σ-point symmetry analysis of ionic displacements in $La_{2-x}Sr_xCuO_4$ shows that the distortion of τ_7 symmetry at the zone boundary, which was invoked to explain the ESR (Ref. 17) and EXAFS (Ref. 15) (Fig. 6), is in fact the zone-boundary (i.e., short-range) equivalent to the τ_1 distortion occuring over a further extended length scale along the Σ direction in the BZ, and the experiments may be detecting the same mode described by Eq. (5).

We end the discussion by noting that the choice of k_0 made on the basis of neutron data also determines the symmetry of the pairing channel in Eq. (5). The first term is isotropic (*s* wave) while the second one has *d*-wave symmetry along the Cu-O bond axes. The relative strengths of the terms are of course to be determined by experiments, but the large phonon anomaly at the Σ point in the inelastic neutron data clearly emphasizes the *d*-wave component.

V. CONCLUSION

The main aim of the present paper is to identify an interaction that can lead to pairing in $La_{2-x}Sr_xCuO_4$ on the basis of a symmetry analysis of the experimentally observed anomalies in the $k \neq 0$ phonon spectrum. It essentially describes the interaction that causes the microscopic inhomogeneities observed in experiments. The rest of the paper is devoted to a discussion of the implications for superconductivity and the phase diagram. The nonlocal Jahn-Teller pairing interaction which couples τ_1 modes at the Σ point with degenerate in-plane O p_x and p_y states is in spirit, if not in detail, similar to the motivation described in the original paper on $La_{2-x}Ba_xCuO_4$ by Bednorz and Müller.[1] The pseudogap in the normal state results from pair density fluctuations, and the temperature T^* represents an energy scale for the pairing $kT^* \sim E_{JT} \simeq 32$ meV for $La_{2-x}Sr_xCuO_4$. The model naturally leads to the formation of stripes and the

crossover from a predominantly paired (bosonic) normal state to a mixed fermion-boson system in the overdoped region. A straightforward and appealing way to explain the doping dependence of T_c in the overdoped regime by Eq. (8) arises from the fact that at higher doping levels, the average stripe lengths increase and thus, *the number of pairs is reduced*, thus reducing T_c. Apart from giving rise to a rather simple phase diagram that is consistent with experimental observations, the model also answers the question of why superconductivity often appears near an orthorhombic phase of the material. However, because the pairs are dynamic and incommensurate, the locally orthorhombic phase associated with the JT pair cannot be easily detected by time- and spatially averaging experimental techniques, and one does *not* expect to observe a static and uniform orthorhombic phase below T^*. On the other hand, the model can explain well the inelastic neutron scattering, neutron PDF, EXAFS, ARPES, susceptibility, and ESR, as well others,[46–48,12] which we have not discussed here.

While here we have mainly focussed on $La_{2-x}Sr_xCuO_4$, we note that similar large $k \neq 0$ lattice distortions have been reported in $YBa_2Cu_3O_{7-\delta}$,[49,50] and we expect a similar mechanism to work there also, as well as the other cuprates and oxides in general where mesoscopic inhomogeneities are observed. We have also omitted a discussion of the spin coupling associated with the local pairs given by the last term in Eq. (5), but mention only that in contrast to the Holstein model, the present Hamiltonian allows the formation of spin singlet *or* triplet pairs.[12] Finally, we might add as a general comment that a short superconducting coherence length of the order of the intercarrier spacing may be an indication that carriers are paired by a finite-wave vector JT instability forming nonlocal pairs. Apart from the cuprates, alkali doped fullerenes might be an example of such a case.

ACKNOWLEDGMENTS

We wish to acknowledge very useful and encouraging discussions with K. A. Müller, V. Kresin, and A. S. Alexandrov, and T. Mertelj for important comments.

[1] G. Bednorz and K. A. Müller, Z. Phys. B: Condens. Matter **64**, 189 (1986).
[2] L. P. Gor'kov and A. V. Sokol, Pis'ma Zh. Éksp. Fiz. **46**, 333 (1987) [JETP Lett. **46**, 420 (1987)].
[3] M. Weger and R. Englman, Physica A **168**, 324 (1999).
[4] R. S. Markiewicz, Physica C **200**, 65 (1992).
[5] V. Z. Kresin, A. Bill, S. A. Wolf, and Yu. N. Ochinnikov, Phys. Rev. B **56**, 107 (1997).
[6] T. Egami, Solid State Commun. **63**, 1019 (1987).
[7] K. A. Muller, J. Supercond. **12**, 3 (1999).
[8] A. Lanzara, Guo-meng Zhao, N. L. Saini, A. Bianconi, K. Conder, H. Keller, and K. A. Muller, J. Phys.: Condens. Matter **11**, L541 (1999).
[9] M. K. Crawford *et al.*, Science **250**, 1309 (1990); J. P. Franck *et al.*, Physica C **185-189**, 1379 (1991); H. J. Bornemann, D. Morris, and H. B. Liu, *ibid.* **182**, 132 (1991).
[10] Guo-meng Zhao, M. B. Hunt, H. Keller, and K. A. Müller, Nature (London) **385**, 236 (1997).
[11] H. A. Mook and F. Dogan, Nature (London) **401**, 145 (1999).
[12] D. Mihailovic, V. V. Kabanov, K. Zagar, and J. Demsar, Phys. Rev. B **60**, R6995 (1999).
[13] R. J. McQeeney, Y. Petrov, T. Egami, M. Yethiraj, G. Shirane, and Y. Endoh, Phys. Rev. Lett. **82**, 628 (1999).
[14] T. R. Sendyka *et al.*, Phys. Rev. B **51**, 6747 (1995).
[15] A. Bianconi *et al.*, Phys. Rev. Lett. **76**, 3412 (1996); N. L. Saini *et al.*, Phys. Rev. B **55**, 12 759 (1997).
[16] E. Bozin, S. Billinge, G. H. Kwei, and H. Takagi, Phys. Rev. B **59**, 4445 (1999).
[17] B. I. Kochelaev *et al.*, Phys. Rev. Lett. **79**, 4274 (1997).
[18] J. Demsar, B. Podobnik, V. V. Kabanov, Th. Wolf, and D. Mihailovic, Phys. Rev. Lett. **82**, 4918 (1999).
[19] K. A. Müller, Guo-meng Zhao, K. Conder, and H. Keller, J. Phys.: Condens. Matter **10**, L291 (1998).
[20] D. Mihailovic, I. Poberaj, T. Mertelj, and J. Demsar, in *Anharmonic Properties of High-T_c Cuprates*, edited by D. Mihailovic *et al.* (World Scientific, Singapore, 1995), p. 148; T. Mertelj *et al.*, Phys. Rev. B **55**, 6061 (1997).
[21] M. R. Norman *et al.*, Nature (London) **392**, 157 (1998).
[22] A *k*-dependent JT interaction, albeit without emphasizing any particular wave vector, was briefly discussed in a different context by K. I. Kugel and D. I. Khomskii, Usp. Fiz. Nauk **136**, 621 (1982) [Sov. Phys. Usp. **25**, 231 (1982)].
[23] F. V. Kuzmartsev, Phys. Rev. Lett. **84**, 530 (2000); see also, A. S. Alexandrov and V. V. Kabanov, Pis'ma Zh. Eksp. Teor. Fiz. **72**, 825 (2000).
[24] Note that a distortion along 45° to the Cu-O bonds (Δ point) is also allowed, but is not discussed further because the experiments suggest that the Σ point is more relevant.
[25] V. V. Kabanov, J. Demsar, B. Podobnik, and D. Mihailovic, Phys. Rev. B **59**, 1497 (1999).
[26] A. A. Alexandrov, V. V. Kabanov, and N. F. Mott, Phys. Rev. Lett. **77**, 4796 (1996).
[27] D. B. Tanner and T. Timusk, in *Physical Properties of High-Temperature Superconductors III*, edited by D. Ginsberg (World Scientific, Singapore, 1992).
[28] A. S. Alexandrov and N. F. Mott, *High-Temperature Superconductors and Other Superfluids* (Taylor & Francis, London, 1994).
[29] Y. J. Uemura *et al.*, Nature (London) **364**, 605 (1993).
[30] A. S. Alexandrov and V. V. Kabanov, Phys. Rev. B **59**, 13 628 (1999).
[31] V. L. Pokrovsky, Pis'ma Zh. Eksp. Theor. Fiz. **47**, 539 (1988) [JETP Lett. **47**, 629 (1988)].
[32] V. J. Emery and S. Kivelson, Nature (London) **374**, 434 (1995).
[33] Of course, formula (8) is an aproximate one. For interacting pairs, it needs to be modified. See for example, V. N. Popov, *Kontinualnie Integrali v Kvantnoi Teorii Polia i Statisticheskoi Fizike* (Atomizdat, Moscow, 1976).
[34] I. Poberaj and D. Mihailovic, Ferroelectrics **128**, 197 (1992); D. Mihailovic and I. Poberaj, Physica C **185-189**, 781 (1991).

[35] D. Mihailovic and A. J. Heeger, Solid State Commun. **75**, 319 (1990); D. Mihailovic, I. Poberaj, and A. Mertelj, Phys. Rev. B **48**, 16 634 (1993).
[36] V. M. Krasnov, A. Yurgens, D. Winkler, P. Delsing, and T. Claeson, Phys. Rev. Lett. **84**, 5860 (2000).
[37] I. G. Lang and Y. A. Firsov, Zh. Eksp. Teor. Fiz. **43**, 1843 (1963) [Sov. Phys. JETP **16**, 1301 (1963)].
[38] A. S. Alexandrov, V. V. Kabanov, and D. K. Ray, Phys. Rev. B **49**, 9915 (1994).
[39] Similar results were obtained by numerical exact calculations with the Hubbard model, where for intersite pairs, the effective mass is of the order of the single polaron mass. See J. Bonca and S. Trugman (unpublished).
[40] A. S. Alexandrov, Phys. Rev. Lett. **82**, 2520 (1999).
[41] G. I. Bersuker and J. B. Goodenough, Physica C **274**, 267 (1997).
[42] B. K. Chakraverty, D. D. Sarma, and C. N. R. Rao, Physica C **156**, 413 (1988); A. S. Alexandrov, Phys. Rev. B **53**, 2863 (1996).
[43] C. Castellani, C. DiCastro, and M. Grilli, Phys. Rev. Lett. **75**, 4650 (1995); A. Perali, C. Castellani, C. DiCastro, M. Grilli, E. Piegari, and A. A. Varlamov, cond-mat/9912363 (unpublished).
[44] D. Mihailovic, T. Mertelj, and K. A. Müller, Phys. Rev. B **57**, 6116 (1998).
[45] For a review see, for example, D. Mihailovic and K. A. Müller, in *High-T_c Superconductivity 1996: Ten Years after the Discovery*, edited by E. Kaldis *et al.* (Kluwer, Dordrecht, 1997), p. 243, and references therein.
[46] J. W. Loram, K. A. Mirza, J. R. Cooper, and J. L. Tallon, Physica C **282-287**, 1405 (1997).
[47] Y. Ando *et al.*, Physica C **282**, 240 (1997); Y. Ando *et al.*, Phys. Rev. Lett. **77**, 2065 (1996).
[48] R. Hackl, in *The Gap Symmetry and Fluctuations in High-T_c Superconductors*, edited by J. Bok *et al.* (Plenum Press, New York, 1998), p. 249.
[49] Y. Petrov, T. Egami, R. J. McQueeney, M. Yethiraj, H. A. Mook, and F. Dogan, cond-mat/0003414 (unpublished).
[50] V. V. Kabanov and Yu. Mashtakov, Phys. Rev. B **47**, 6060 (1993).